Thesis for The Degree of Licentiate of Engineering

Numerical Modelling and Ultrasound Velocity Profiling of Wood Chips Flow in an Industrial Application

Sofia Evysdotter

Department of Chemistry and Chemical Engineering
Chalmers University of Technology
Gothenburg, Sweden, 2025

Numerical Modelling and Ultrasound Velocity Profiling of Wood Chips Flow in an Industrial Application

Sofia Evysdotter

Technical Report No 2025:02

Department of Chemistry and Chemical Engineering
Chalmers University of Technology
SE-412 96 Göteborg,
Sweden
Phone: +46(0)31 772 1000

Printed by Chalmers Digitaltryck,
Gothenburg, Sweden 2025.

Numerical Modelling and Ultrasound Velocity Profiling of Wood Chips Flow in an Industrial Application

Sofia Evysdotter

Department of Chemistry and Chemical Engineering
Chalmers University of Technology

Abstract

Large amounts of energy and raw material are required to produce pulp and understanding the process and equipment is the key to optimization of energy consumption as well as chemicals and overall yield of the process. Conducting experiments on lab-scale for impregnation vessels remains a challenge and a numerical model enables a cost-effective test environment where to gain insight of the complex process. In this work a *computational fluid dynamics, CFD model* is examined. The solid and liquid phases were both treated as continua, and it was found that the continuum model for the solid wood chips phase could capture the previously observed oscillating formation of arches in the contracting part of the vessel. This has been observed in more refined models, for smaller particle systems, which are not feasible for industrial-scale pulping equipment. The present work also highlights the importance of correct material data when using the model as a design tool. As an initial step to validate the models for wood chips flow, *Ultrasound Velocity profiling*, UVP measurements were performed on an industrial impregnation vessel. The measurements could successfully capture the velocity of the wood chips and the normal production variation at the mill. The velocity profiles of the wood chips show a non-zero velocity at the wall, a shear zone and a plug flow, which indicates that the wood chips flow can be regarded as a dense granular flow and the rheology can be described with the Bingham fluid model and that the partial slip condition could be used to model the interaction with the wall.

Keywords

CFD, multiphase, wood chips flow, dense granular flow, industrial scale, UVP

List of Publications

Appended publications

This thesis is based on the following publications:

[**Paper I**] **S. Evysdotter**, T. Vikström, A. Rasmuson, *Parameter sensitivity of a wood chips flow model*
The Canadian Journal of Chemical Engineering 103 (2025), 868-879.

[**Paper II**] **S. Evysdotter**, A. Rasmuson, T. Vikström, *Ultrasound velocity profiling of wood chips flow in an industrial application*
manuscript.

Contribution report

Paper I First author, responsible for numerical modelling, writing and revision. Results were analyzed together with co-authors.

Paper II First author, responsible for writing, planing the measurements, and analyzing the data.

Acknowledgments

I would like to express my deepest gratitude toward my supervisors Professor Tomas Vikström and Professor Anders Rasmuson for their engagement and for making this project possible.

Special thanks to the following, whom without this would not have been possible:

The personnel at SCA Östrand for their patience and help during the UVP-measurement.

Everyone at Incipientus and especially Tommy Andersson and Doctor Johan Wiklund for help with the UVP-measurements.

My colleague Rasmus Müllback for the custom designed bracket.

The Swedish Energy Agency and Valmet AB for funding.

Contents

Chapter 1

Introduction

1.1 Background

Around 100 A.D the Chinese invented the ability to unite random fibers of disintegrated plant tissue or fabric pieces into smooth sheets. Before this, mostly papyrus and parchment were used for writing none of which are defined as paper. The paper made from disintegrated and pressed fibers were more economical and durable and had an even surface. Nowadays, pulp of wood can be used for many different products, such as printing paper, tissue paper, cardboard, fabric and as a replacement material for plastic.

Sweden is a major exporter of forest products in the world [1]. The pulp and paper industry is a large part of the Swedish economy and it also consumes a considerable part of the electric energy consumed by industries in Sweden. Every improvement that can reduce the energy consumption of the pulp making is thus welcome both from an environmental as well as from an economic aspect.

Fibrous material pulp can be produced either chemically, mechanically, or via a combination of both, using a lignocellulosic raw material such as wood or straw. Wood is mainly made up of cellulose, hemicellulose, and lignin, all which are large polymers. To separate the fibers in order to make pulp, the lignin, which provides compressive strength and waterproofing of the cell walls, must be dissolved. The present thesis is focused on the equipment used in chemical pulping with wood as raw material. The chemical delignification process is carried out in either batch or continuous digester vessels with the assistance of sodium hydroxide, sodium sulphide and heat. The purpose of the delignification is to dissolve the lignin, this must be carefully performed in order to produce a strong pulp at high yield. The desired level of delignification depends on the final product. Dissolving the lignin is not solely to free the fibers, it is also an important step in the bleaching process of the pulp. Reducing the amount of lignin early in the pulping process saves bleaching chemicals later on. During the delignification process, carbohydrates are unfortunately simultaneously dissolved, this is not a desired reaction, since it decreases the yield and strength

of the pulp. Measuring the yield in the pulping process is done by taking the ratio of oven dry pulp to oven dry input. A typical value of the yield is around 50 %. The degree of delignification is expressed by the Kappa-number which states the amount of residual lignin and the final Kappa number of the pulp leaving the digester is in the range of 25-35 for soft wood and around 16-23 for hard wood.

Kraft pulping is a highly complex process where the fluid-dynamics of a multi-component multiphase flow interact with the chemical kinetics via mass and heat transfer in a large vessel. To fully comprehend the situation prevailing in the digester vessels, the mass, heat and momentum transport in three dimensions must be taken into account. The way the solids are packed depend on their properties, chips with high kappa number are stiff and do not easily deform compared to chips with low kappa number. The kappa number affects the solid pressure in the vessel which in turn affects the distribution of solids and liquor in the vessel, which in turn again affects the kappa number of the chips. From this it is understood that both the chemical reactions, mass and heat transfer as well as the fluid dynamics must be well understood and considered at the same time since they interact.

There are large differences in the length scales of the various physical phenomena which take place in a pulp digester. The vessel size has increased over the last years which raises the needs for better understanding of the fluid dynamics and mass and heat transport in three dimensions in the vessels to ensure an even quality of the pulp. A pulp digester can be as large as up to 14 m in diameter and the smallest dimension of a single chip is a few millimeters. The chemical reactions and kinetics of the delignification process are rather well understood on the scale of the chips. The hydrodynamics as well as the heat and mass transfer prevailing in large pulping vessels are not and the size itself of today's equipment imposes new challenges.

Depending on the final product, the unit operations and the equipment needed vary to some extent. Most of the pulp produced today is chemical pulp, in this process the raw material is boiled together with an alkaline fluid in a pulp digester which can be both continuous and of batch type. Here follows a description of a continuous cooking system with wood as the intended material. This section is based on [2].

The continuous cooking equipment can be one vessel or two vessels. If the cooking equipment consists of two vessels, the first one is utilized for impregnation of the raw material. The impregnation can also be performed in the top of the digester, as in a one vessel system. Regardless of one or two vessels, the cooking process can be divided into the following stages:

- Feeding of raw material
- Pre-steaming
- White liquor charge

- Impregnation
- Heating
- Washing
- Blow line feed

The first step is pre-steaming, which is often performed in two consecutive stages, one at atmospheric pressure and one at over pressure with the aim at filling the pores with steam that later condenses. It is highly important that the wood chips are sufficiently pre-steamed since otherwise air will remain in the pores of the wood chips. This will cause the wood chips to be more buoyant and also the mass transport of the chemicals will be negatively affected.

As the next step, wood chips and white liquor are fed to the impregnation zone or separate impregnation vessel. The separate impregnation vessel resembles a somewhat smaller digester and the residence time is about one hour in approximately 90°C and atmospheric pressure. During the impregnation the charged alkali is transported into the reactive sites and the chemical degradation of lignin and carbohydrates is started, however slowly, dependent on temperature. The mixture of wood chips and liquor is further fed to the digester (in the case of a two-vessel system) using a high-pressure pump. In modern continuous cooking systems, the alkali charge is divided into three occasions, the first one is into the impregnation vessel. After the chips and liquor mixture are transferred from the impregnation vessel to the digester the second charge of white liquor is executed.

The main part of the delignification occurs in the co-current zone in the top of the digester, further down the third alkali charge is done in the counter-current cooking zone. In the bottom of the digester is a washing zone. In the washing zone the washing liquor flows counter-current to the chips column and displaces the cooking liquor. A few percent of the alkali charge can be done in this zone. Together with external heaters, this has prolonged the cooking zone in the digester to its full length and has resulted in that the whole cook can be conducted at a lower temperature and yield a pulp with lower kappa without losing strength. As in the impregnation vessel the pulp is ejected in the bottom.

There is research regarding only chemical reactions of the pulping process as well as work regarding only the flow field in packed columns. In the case where both are considered, the complexity of either one is often reduced, by assuming one dimensional flow or less detailed reaction pattern. Understanding the combined effect of the physical and chemical phenomena occurring in an impregnation vessel and following pulp digester can lead to more optimized performance and operation. This will increase yield, produce an even pulp quality and reduce waste. Understanding the hydrodynamic situation in the cooking system will help in reducing the risk of malfunctioning behavior such as channeling and fouling.

1.2 The impregnation vessel

In this work, an example of a type of impregnation vessel, which is a part of a two-vessel continuous cooking system will be studied. There are several other versions of similar large vessels used for pulping. The impregnation vessel precedes the digester and is utilized to impregnate the wood chips with cooking liquor. A schematic picture of the impregnation vessel studied is given in Figure 1.1. First, steam is added to remove the air in the chips; second, the cooking liquor is added but the temperature remains rather low, keeping the reaction rate slow. The vessel includes two screen packages, at positions 2 and 3, where liquid is extracted for circulation and two vertical positions of injection points, Figure 1.1, positions 4 and 5; the chips are fed into the vessel in the top and 2 m above the screens is the liquid level, position 1, hence the impregnation vessel is not completely filled with liquid. The cooking liquid is fed into the vessel at the top and also at the two injection positions, which are placed around the spherical part of the bottom for the current geometry, to dilute the outflow. The upper injection point is located at the intersection of the spherical bottom and the upper cylindrical part. The lower injection point is located at a radius of 3.2 $[m]$.

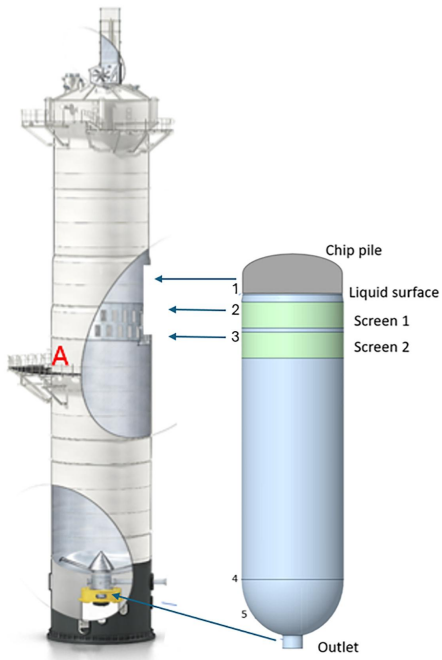

Figure 1.1: The impregnation vessel; diameter = 8.8 m, height = 46 m, liquid level = 24 m above spherical part, outlet diameter = 1.75 m. Left side, a 3D-rendering of the complete impregnation vessel, with the measuring point A marked. Right side, the computational domain, 360 degrees.

1.3 Objectives

The objective of this thesis is to develop a computational fluid model which can describe the flow behavior of wood chips and the momentum transfer in an adequate manner in order to capture the key features and phenomena occurring in industrial scale pulp mills. An accurate model of this type can be used to conduct numerical experiments where the large-scale problems of this equipment can be analyzed, something that is challenging in lab-scale equipment. To be able to further extend this model of wood chips to include mass and energy transport as well as chemical reactions which describe the delignification process occurring in the cooking system a *Computational Fluid Dynamics*, CFD model will be applied.

Utrasound Velocity Profiling UVP, will be used to measure the velocity profile of the wood chips in an impregnation vessel. The data from the ultrasound velocity profiling can be used to validate the boundary conditions for the CFD models and give insight into whether it is reasonable to model wood chips on industrial scale as a dense granular flow.

1.4 Outline

Chapter 2 gives a theoretical background to modelling particle-particle interactions and the development of arches, which particulate matter can exhibit. Further, previous work regarding numerical modelling of industrial pulping equipment is presented. In Chapter 3, the numerical models for computational fluid dynamics, CFD are presented. The theory of ultrasound velocity profiling is briefly described in Chapter 4, as well as some previous applications. Chapter 5 presents the result from the numerical simulations and the ultrasound measurements. Chapter 6 provides a discussion regarding the numerical results as well as the experimental, and the connection between them. In Chapter 7 the conclusions from the numerical and experimental results are presented. Further work is discussed in Chapter 8. The two papers are attached.

1.5 Included papers

Paper I

Parameter sensitivity of a wood chips flow model describes a sensitivity analysis with CFD, computational fluid dynamics, of important model parameters for describing flow of wood chips.

Problem

To optimize the chemical charge into the impregnation vessel and operation, the flow field must be well understood. To be able to predict how much chemicals each wood chip is subjected to, the presence of the wood chips must be known, hence the most crucial parameters in the modelling of cooking system are the distribution of wood chips and the material properties which effect the distribution. This also affects the operation of the equipment, and insight into how the wood chips are distributed can help prevent malfunctioning.

Contribution

This paper contributes to the understanding of the complex behavior of the flow conditions of wood particles in large vessels. The continuum model examined can capture the oscillating phenomena of forming and debilitating arches, previously seen in more refined particle models. The continuum models' ability to capture the same behavior enables the possibility to model large systems. Further, paper I examines how the material properties of the wood chips enhance or reduce the oscillations in pressure and formation of arches.

Paper II

Ultrasound velocity profiling of wood chips flow in an industrial application presents ultrasound velocity profiles from an industrial impregnation vessel.

Problem

The conditions on the inside of industrial impregnation vessel and pulp digester are unknown and not easily attainable due to the basic fluid and high temperature. Industrial reactors of this type are typically very large, with diameters approximately from 4-12 m, and thus it cannot be assumed that lab scale equipment experiences the same flow pattern, which further emphasizes the need to investigate the actual industrial equipment. It is crucial for the operation and optimization of this type of equipment to gain insight about the flow field.

Contribution

This paper presents results from UVP, Ultrasound Velocity Profiling, conducted on an industrial impregnation vessel. The presented results show that it is possible to measure the velocity of the wood chips through the 15 mm thick steel wall and capture the normal variations of productions occurring in the mill. Further, the measured velocity profiles showed that the wood chips exhibit the behavior of dense granular flow when interacting with the wall. A non-zero velocity was found at the wall, followed by a small shear zone and then plug flow.

Chapter 2

Particle flow and solid pressure

In this chapter the theory of particle flow and solid pressure will be presented, as well as specific features and previous modelling work of similar equipment and granular flow. Some suitable examples in which similar phenomena to the ones existing in the impregnation vessel will be discussed phenomenologically.

2.1 Particle flow

A cooking system can consist of one or two vessels, in the later configuration, the first vessel is used for impregnation of the wood chips with cooking liquor. Both the impregnation vessel and the continuous pulp digester show some similarities to a packed bed of solids in which a fluid is passing, in the sense that the packing of solids in the vessel affects how the liquid is distributed. Even though the chips are also moving, they do not move around freely in the liquid phase but are in contact with each other when the volume fraction exceeds a critical value, this is referred to as degree of packing 1 and can be observed when wood chips are poured into a stack on the ground. In this type of industrial vessels, the volume fraction of chips is unknown but can be estimated by the load of the column of wood chips and a constitutive equation for the interaction between the wood chips. Perhaps the most crucial property of this type of equipment to predict is the distribution of the solid phase, the chips. This will determine how the liquor moves through the solid body made up of chips which determines to what extent the chips are being subjected to cooking chemicals etc. This is further complicated by the fact that the flow of the fluid phase also affects the solid distribution where liquid flow can disrupt the network formed by the wood chips. There are three major approaches to treat this problem, depending on which questions one wishes to answer. One approach is to describe each particle using Newtonian mechanics, Discrete Element Modelling, DEM. This method is too limited in the number of particles which can be considered for modelling industrial scale digesters. It

also remains a challenge to incorporate mass transfer and chemical reactions which are needed for a full-scale total model of a pulp digester system. Another way is to describe the solid phase as a continuum on the macroscopic scale, this requires further modelling for closing the governing equations. In this work this method will be utilized. A third way, which would be a further simplification would be to regard the solid phase as a porous body.

When a significantly large number of particles are present their behavior can be described as a continuum on the macro scale. This can be observed in an hourglass in which sand is "flowing" or in a pulp mill where the dry chips are poured onto stacks. Each individual wood chip is a discrete object and large enough to be described by Newtonian mechanics. However, macroscopically the wood chips assembly may be regarded as a continuum. This duality is characteristic fo granular materials and the properties at the continuum scale are governed by the grain scale. When characterizing particle flow, the particle velocity and the density of the interstitial fluid should be considered. If the density of the particles is much larger than the interstitial fluid the effect of the momentum transfer from the fluid can often be neglected, which simplifies the fluid dynamics of the granular matter from a multi-phase process to a single-phase process, Campbell [3]. If the velocity of the particles is rapid, the flow is dilute and the particle-particle interactions are characterized by binary collisions, the modified theory of gases is commonly used to describe the situation, [4]. Further, if the inertia of the particles can be neglected there is a quasi-static regime which is represented by soil plasticity models [4]. The third regime of particle flow is the slow-moving dense flow, where the inertia of the particles is no longer negligible and the particles are in constant contact with each other, forming a network. For the application of the impregnation vessel, the particles are in contact with each other and move slowly downwards due to gravity and the density of the interstitial fluid is in the same order of magnitude as the density of the particles. The behavior of granular materials is dependent on the local stresses which it is subjected to, and it can exhibit both solid and fluidlike properties. The particle pressure between the particles enables it to resist loads and can thus support structures and be poured into stacks with a material specific angle of repose, behaving as an elastic solid, as described by Campbell [3]. If the load exceeds the particle pressure, the granular material starts to move and exhibit fluid like properties. This, the yield criterion, is described by Jop et al [5] as a key feature of granular flow together with the complex relation to shear rate in the flowing state. Depending on the rate at which the movement of the particles develops, particles can stay in contact with each other and sustain some of the frictional force and will stay this way as long as the rupture is at moderate pace. The microscopic properties of each individual particle, such as shape, surface friction and polydispersity effects the flow behavior of the granular material on the macroscale according to Mueth [6], [7]. This is also the characteristic behavior of visco-plastic fluids such as Bingham fluids. Another similarity to Bingham fluids is the interaction with the wall. Granular materials differ from conventional fluids, in general, granular matter exhibits a slip condition at a wall boundary, and according to Campbell [3], the slip is dependent on the interaction between the granular flow and the

boundary. Since there is a slip condition the boundary acts a source of shear equal to the product of the wall shear stress and the slip velocity [3].

Granular material also shows similar plastic behavior as metals, they exhibit yield stress and close to rate independent plastic deformation. In addition to this, granular materials also have a relatively substantial dependence on volume fraction and pressure alterations. By increasing the solid pressure on a granular material an irreversible deformation and volume change can occur. A volume change of the granular material can both harden and soften the aggregation. However, granular material differs from metals because the plastic deformation is not incompressible, which for metals mean that as they plastically deform, and the atoms shift, the volume do not change. For a body of wood chips, the volume can change as the particles shift due to shear and plastic deformation. Another important feature of granular materials is the dilatancy, which together with the frictional resistance are two key properties on the grain scale which are needed for the macroscopic description. The dilatancy arises under shear stress when the particles which are interconnected in a consolidated state move and produce a bulk expansion of the material. The overall plastic deformation of granular materials is a result of both the plastic deformation of individual grains as well as persistent rearrangement. When modelling compaction and deformation of granular material constitutive equations for the elasto-plastic behavior is needed. The force per unit area needed to deform a solid material is the E-modulus and together with the yield, these two parameters describe the elasto-plastic properties of a granular material and the interactions of the particles at a macroscopic scale.

2.2 Solid pressure

The flow through a network of solids exerts viscous shear stresses on the said network which causes it to deform and consolidate, this is called poro-elasticity and is a phenomenon where fluid flow and solid network deformation are coupled. For the network to form, a minimum amount of solids must be present. This is measured in volume fraction and referred to as gel point, critical volume fraction or sedimentation concentration, de Kretser et al. [8], and corresponds to where the amount of particles is high enough so that they do not move around freely but are in contact with each other. When this point is reached, the interaction resists gravity and compression and results in an additional stress term in the force balance. The additional stress term is related to the particle pressure P_s, which is associated to the elastic stress of the network, according to de Kretser [8]. Because of this, the force balance should be made over a volume element rather than on a single particle.

The constitutive equation for P_s could be related to the volume fraction φ and the velocity u. The network strength which depends on the local volume fraction is referred to as the compressive yield stress. As an element of the network is subjected to an applied stress, it will remain in the original state

until the applied stress exceeds the yield stress. When the yield stress is exceeded, the network deforms, and the solids consolidate which results in an increase in the local volume fraction. If the applied stress is relieved, the network does in general not transform back to its original form.

MacMinn et al. [9] conducted experiments using hydrogel spheres placed between two discs where a mixture of water and glycerol was injected. A continuum model for the process of poromechanical deformation was derived. The contact of the particles are Hertzian, they are incompressible (Poission ratio 1/2) and soft (Young modulus 20 kPa), elastic and non-cohesive. Further assumptions in the model is conservation of volume (Incompressible means that the particles can rearrange and deform but their volume will not change), the stress and pressure gradients in the fluid and in the solid skeleton are poromechanically coupled. Elastic energy is stored in the solid skeleton and there is viscous dissipation due to rearrangements. It is further assumed that the skeleton formed by the solids stores elastic energy due to volume compression but not due to shear and hence isotropy is assumed. A non-linear conservation law for the porosity as a function of time can then be formed which includes the stress in the solid skeleton. In the poroelastical theory, the pressure gradient in the fluid act as a body force on the solid skeleton. To solve for the porosity of the system a constitutive law relating the strain to the stress for the solid skeleton is needed. As the stress is taken to be Hertzian elastic and linearly viscous it can be written as:

$$\sigma'(\phi_f) = \mathcal{K}\tilde{\phi_f}|\tilde{\phi_f}|^{1/2} + \mu\frac{\partial\tilde{\phi_f}}{\partial t} \tag{2.1}$$

where, $\mathcal{K}$ and μ are the effective bulk modulus and viscosity of the solid continuum phase and $\tilde{\phi}_f$ is the normalized change in porosity. In the experiments, particle rearrangement and hysteresis are observed.

In 2016 Hewitt et al. [10] studied flow of water through a porous deformable media consisting of hydrogel spheres, where the flow was driven by a pressure head. Because the spheres were buoyancy neutral the only compacting force is the one arising from the fluid flowing downwards. It was observed experimentally that the flux does not increase linearly with increasing pressure, instead the flux increases towards a finite maximum, which is attributed to the fact that the hydrogel spheres are deformable. Further it was found that the bed height is compacted to an asymptotic finite value, and this leads to that the effective permeability decreases towards zero. The conclusion is that the flux through deformable media can be insensitive to large applied fluid pressure. Increased pressure gradients are balanced by increased resistance from permeability and thus the flow is self-regulated. As the authors argue, there is a key difference between compaction driven by an external load or by fluid flow and that is that in the latter case, there is a gradient in the fluid pressure which results in a gradient in the porosity. The model presented by Hewitt et al. [10], fails to capture the experimentally observed hysteresis effect in the compaction procedure. As the pressure was decreased, after first being increased, the

particles could not revert completely, they had a strong dependence of the previous state of compaction. The constitutive equation for the solid interaction, referred to as the matrix pressure is dependent on the strain and elasticity modulus. The strain in turn, depends on the porosity, void fraction, φ.

$$\frac{\sigma}{\sigma^*} = -\frac{e}{1 - e/e_m}$$
$$e = \frac{\varphi - \Theta}{1 - \varphi} \tag{2.2}$$

where e_m is a limit of the strain which the solids cannot be compacted beyond and σ^* is the elastic modulus. Θ is the uniform porosity, corresponding to zero strain on the solid matrix.

When a porous media is subjected to a stress such as compression, shear or deformation, according to Terzaghi's principle the relationship between the effective stress, total stress and pore pressure is as follows:

$$\sigma = \sigma' + u \tag{2.3}$$

This equation is valid under the assumptions that the porous media is isotropic and the incompressible particles constituting the media are saturated. The strains in the media should also be small and Darcy flow should apply. Also, the permeability should be constant during the process and the unique relation between the total stress and the void fraction is independent of time. Terzaghi developed this relationship under these assumptions for saturated soils. For the impregnation vessel, this means that as the solid pressure increases the hydrostatic pressure decreases.

2.3 Approaches for modelling of wood chips flow

Considering a relatively small number of wood chips, one would resort to discrete element modelling when attempting to describe how they interact if contained in a vessel. Modelling particle interaction with DEM has been applied to a vast number of situations. In the pulp digester non-uniform particles are exerted to uniaxial compaction due to gravity, liquor flow and weight from feeding of solids. Gan and Kamlah [11] modelled the uni-axial compaction of ceramic pebbles using DEM where they relate the contact forces of particles to the macroscopic stress tensor to describe how the spherical particles are compacted. The macroscopic strain was applied, and the stress calculated from the interaction forces. The elasticity modulus of the pebbles depend on the temperature and porosity as follows:

$$E = 110(1 - \tilde{p})^3(1 - 2.5e^{-4}(T - 293)) \tag{2.4}$$

In experiments and simulation macroscopic irreversibility is observed when the particle assembly is unloaded, even though the particles are purely elastic.

This behavior of the particle assembly can only be explained by rearrangement of the elastic particles.

Modelling granular media with continuum models has historically been of large interest in soil mechanics. These models are sophisticated and capture many of the complex properties of the granular material which can be observed as well in soil as in piles of wood chips. Both cases can be seen as a porous material with pore fluid in the interconnected pores between the granular solids. According to Chen and Baladi [12] for this type of two-phase continuum the stress component can be divided into two parts, one connected to the solid matrix, and one connected to the pore fluid, that is the pore pressure. The strength of the granular material arises from the interlocking particles, if the pore pressure increases, the strength of the granular material decreases by pushing the particles away. In addition to incompressible plastic deformation wood chips exhibit shear strength hardening as the particle pressure increases. It behaves both elastic and plastic, and the elastic part is most likely non-linear. The stress-strain curve should be progressive, meaning that the material hardens as it is compacted. Both shear and compaction can result in flowing. A model that can deal with all these properties is the Drucker-Prager model with a CAP or the Cam Clay model which has a pressure dependent yield condition, Pettersson and Pettersson [13]. Both numerical simulations and experiments of chips compaction were performed by Pettersson and Pettersson, and it was concluded that the Cam Clay model describes the behavior of the compaction of wood chips well.

The most widely used model for solid interaction in pulp digesters is the model developed by Härkönen [14]. The column of wood chips in the pulp digester is elastic and compressible, which greatly affects porosity. To account for this Härkönen defines the solid pressure, which models the interactions between the particles since the vast number of particles inhibits the possibility to define this force exactly. By conducting laboratory experiments on wood chips an expression for the solid pressure as a function of the Kappa-number and volume fraction was developed. An expression for the flow resistance was also developed where the coefficients of the Ergun equation were modified to account for the irregular shape of the wood chips. The expression developed by Härkönen which relates the solid pressure to the volume fraction and Kappa-number is according to Equation 2.5

$$\varphi_2 = k_0 + P_s^{k_1}(k_2 + k_3 ln(\kappa)) \tag{2.5}$$

where κ is the kappa number which describes the degree of delignification.

The flow resistance in porous material is determined by Darcys law:

$$\frac{dP}{dx} = \frac{\mu}{k}\nu \tag{2.6}$$

where k is given by Kozeny-Carman relation for laminar flow.

$$k = \frac{\varphi^3}{\theta s_v^2 (1-\varphi)^2} \tag{2.7}$$

A general form of describing the flow resistance through a porous material is the Ergun equation which is valid also for "turbulent" flow regime. The Ergun equation is:

$$\frac{\Delta p}{\Delta x} = R_1 \frac{(1-\varphi_2)^2}{\varphi_2^3} v + R_2 \frac{(1-\varphi_2)}{\varphi_2^3} v^2 \tag{2.8}$$

The constants in Härkönens modified Ergun equation have been under investigation by several authors. In 2002 Lee [15] conducted experiment on a laboratory scale column of packed wood chips. The pressure drop was measured against superficial velocity, kappa, void fraction and compacting pressure and it was concluded that Härkönens constants in the equation for the pressure drop are too small. Also, the constants should not be universal constants since the shape and size of the solids in the bed greatly affect the pressure drop. The constants for uncooked chips do not predict the pressure drop of cooked chips, since the pressure drop is largely dependent on the void fraction of the bed which in turn is dependent on the kappa number, which is linked to the elasticity modulus of the column which also affects the compaction, and all this combined affects the drag force. The void fraction is not evenly distributed over the column and correlations based on the average void fraction are likely insufficient in predicting the pressure drop.

Further work regarding the coefficients of the flow resistance and solid interaction was done by Alaqqad et al [16] who investigated the effect of the compressibility on the permeability of a bed of wood chips. The general equation for the solid stress term is:

$$p_s = m(\varphi_g - \varphi)^n \tag{2.9}$$

where the coefficient m is usually dependent on the Kappa-number for wood chips and corresponds to the stiffness of the network. φ_g is the gelpoint, the exponent n as well as m are empirical constants. In the equation describing the permeability, Equation 2.8, the constants R_1 and R_2 models the lumped effect of tortuosity and specific surface of the solid distribution as well as the density and viscosity of the fluid. Alaqqad presents a list of previous investigations of the parameters R_1 and R_2. For more details the reader is referred to [16]. Their own method which accounts for the compressibility effects of the bed predicts a smaller pressure drop through the bed of wood chips.

Lundström [17], performed measurements on fiber beds and have shown that the permeability in the plane is an order of magnitude higher than out of the plane. The measurements as well as the simulations regarding the permeability in a bed of chips are all one dimensional. In an equipment such as an impregnation vessel or a pulp digester where the conditions are three

dimensional due to extraction and dilution, a reasonable approach would be to not assume isotropic permeability. The permeability is also affected by flow induced compaction Weitzenbock [18] and thus not constant through the chip-bed.

The model of Härkönen lacks the frictional properties of the solid phase. By describing the wood chips as granular flow, Djebbar et al. [19] implements the Mohr-Coulomb criteria for the visco-plastic behavior of the granular phase as shear viscosity, which is a function of the solid pressure, friction angle and the rate of deformation. Further is the friction between the walls and the wood chips also a function of the solid pressure. The authors compare 2D CFD simulations of Härkönens model with CFD simulations of Härkönens model together with the Mohr-Coulomb criteria. It is concluded that the frictional properties of the solid phase have a significant impact on the pressure field in the reactor. However, the authors present pressure fields from the frictional case which are not in accordance with the knowledge from the industry. The pressure drop over the reactor is significantly lower than reported for industrial digesters. Also, the profile of the pressure is not concordant. The highest pressure in the industrial reactors is near the extraction screens and not in the bottom as reported by Djebbar et al. [19]. The authors mention that the walls of the reactor influence the pressure profile, they however fail to mention that in their model the wall friction is probably highly overestimated which can be seen in the velocity profile they present, where the boundary layers are unreasonably thick.

Studying Equations 2.1 2.2, 2.4, and 2.5, the similarities are noted, all depend on the porosity of the material. At the macroscopic level, regarding the complete body of wood chips as a porous particle, the elasticity modulus of the ceramic pebbles in Equation 2.4 and the solid pressure of Härkönen are analogous. The solid pressure model by Härkönen may be thought of as a black box model of what is happening to the wood chips at the micro scale. They rearrange, deform and most likely also collapse to some extent. Each individual step is not measurable on the macro level of the bed of wood chips. Wood chips are irregularly shaped, compared to the spheres examined by de Kretser et al, and it is important to recognize that when modelling compression of irregular shaped particles they can rotate, rearrange and deform. The logarithmic profile of the solid pressure by Härkönen suggest that the flat start of the curve are accounts for the rearrangement of the particles and as a larger force is needed to compact the bed more, the curve tangents the elasticity modulus of the wood components. Coming from different starting points all models end up with similar ways of describing how the solids interact and are compacted. However, the number of particles in an impregnation vessel is to vast for a *Discrete Element Model*, DEM, and the ability to extend the model with temperature fields and mass transport is limited. The momentum transfer from the fluid phase does also have to be accounted for and the remaining way of describing the two interacting phases is the Eulerian multiphase model.

2.4 Arching

The impregnation vessel is geometrically similar to storage tanks, silos, used for agricultural material, which are also granular materials. Due to these two common features, the impregnation vessel can exhibit a phenomenon commonly observed in silos, called arching. Drescher et al.[20] refer to *arching* as

> the spontaneous formation of an arch-like supported stagnant mass of bulk material in a bin or hopper upon opening of the outlet or during gravitational flow.

It is further stated that the formation of arches depends on the geometry and the ratio of the outlet size to the vessel size. As for architectural arches, these can hold up the load of the material above, which Hidalgo et al. [21] analyzed using DEM. Hinterreiter et al. [22], stated that factors that affect the tendency to form arches, for wood chips, are the shape, size, and aspect ratio. These are highly important in understanding the arching phenomena. An arch is typically formed adjacent to the outlet. Yoshida [23] found, using DEM, that the periodicity of the pulsation of the particles in the upper part of the silo is identical to the variations in pressure on the silo walls, which long have been thought of as a result of the formation and collapse of arches. Arches that form at a bottleneck are a large problem when clogging or jamming occurs, To et al. [24] examined the probability of jamming due to convex arch formation in 2D-silos.

2.5 Previous Work

One of the first to combine the hydrodynamics of the pulp digester with modelling of the delignification was Saltin [25]. Saltin modified the hydrodynamic equations by Härkönen [14] to a dynamic one-dimensional model which is able to predict data from the literature. Michelsen and Foss [26] also created a one-dimensional model in 1996 where the interactions between the axial flow and the chemical reactions were considered [26]. They use a simplified version of the Purdue model by Christensen [27], and extended the reactor modelling by considering axial momentum transport in a simulated industrial digester. Solid interaction and wall behavior are functions of the solid pressure according to Härkönen. The importance of the interaction between the momentum transport and the kinetics is well displayed by the effect on the kappa number by the residence time.

Wisnewski, Doyle III and Kayihan [28] used a Continuous Stirred Tank Reactor, CSTR, approach where the compaction of the wood chips along the digester height is assumed to be known. In the work by Fernandez and Castro [29] a predefined axial compaction of the wood chips in the digester, which is modelled by mixing cells, this reactor model can predict the total solids content which is an industrially important parameter. Bhartyia et el. [30] combined the work by Wisnewski [28] in 2003 with the work done by Michelsen

[26]. The result is a model with axial momentum transport and rather complex kinetic pattern. By doing this the authors were able to model grade transition since the chip compaction and chip level are included in the model. The radial gradients are neglected, and it is assumed that the solid and liquid phases are in thermal and dynamic equilibrium. Pourian [31] modelled an industrial pulp digester using the Eulerian multiphase approach using CFD. The model is two-dimensional with rotational symmetry. The bed of chips is divided into sections where the predetermined porosity is changing. Pourian also investigated the effect of channeling by adding artificial channels to the chip bed and found that, not suprisingly, less reaction occurs in the channels due to the increased velocity of the liquor.

He et al. [32] proposed a CFD-model which is a combination of Härkönens chips compaction model and Michelsens assumptions. Pougatch et al. [33] developed a two-dimensional model with rotational symmetry of the reacting flow in a pulp digester. The simulated geometry is a 30° piece of the cylindrical reactor. In this model the two-dimensional flow is combined with the somewhat simplified kinetics of Michelsen, [26]. A further development is that the solid phase is regarded as a Bingham fluid with the yield stress of the viscosity as a function of the solid pressure, which is modelled according to Härkönen, [14]. Also, the interaction between the walls and the solid phase is dependent on the solid pressure. In this model the compaction of the chips is rather uniform except near the injection points. Fan [34] continued on the model by Pougatch and examined the effect of particle size on chips compressibility using CFD in an industrial digester, the computational domain was simplified to not include the complex bottom part. It was found that the compressibility of the chips significantly affects the cooking performance due to the effect on the residence time.

Rantanen [35] combined the kinetic model developed by Gustafson [36] and the solid pressure function developed by Härkönen [14], which results in a model that uses the real time modelled profiles of chemicals, temperature and solids concentration to model the packing degree of the reactor. Laakso [37] set up a model of a continuous kraft cooking digester with the hypothesis that a chip bed packing model can solve the residence time and process conditions in the digester, which in turn affect the delignification, which in turn affect the packing. Laakso utilizes the model by Gustafson for reaction kinetics in combination with the model by Härkönen for the chip bed pressure. The residence time for various values of coefficients in the Ergun equation are compared to mill data.

Chapter 3

Computational Fluid Dynamics Model

In this section the numerical models for the computational fluid dynamics, CFD, simulations will be presented.

3.1 Governing equations

In order to model this multiphase system with dense particle loading and where the focus of this work is on the hydrodynamic conditions, the Euler–Euler method was chosen; due to the number of particles, the Lagrangian approach is not applicable. The Euler–Euler method treats all included phases as interpenetrating continua. The following equations constitute the inhomogeneous model, which allows for the phases to have separate velocity fields, that has been used in this work.

$$\frac{\partial}{\partial t}\left(\varphi_\alpha \rho_\alpha\right) + \nabla \cdot \left(\varphi_\alpha \rho_\alpha \mathbf{U}_\alpha\right) = \mathbf{S}_{MS_\alpha} + \sum_{\beta=1}^{N_p} \Gamma_{\alpha\beta} \tag{3.1}$$

In Equation 3.1, the continuity equation, the first term on the left side is accumulation, the second term is the convective transport where $\mathbf{U}_\alpha$ is vector velocity. On the right-hand side the first term denotes the user specified mass sources and the second term is the mass flow rate per unit volume from phase β to α.

$$\begin{aligned}\frac{\partial}{\partial t}\left(\varepsilon_\alpha \rho_\alpha \mathbf{U}_\alpha\right) + \nabla \cdot \left(\varepsilon_\alpha (\rho_\alpha \mathbf{U}_\alpha \otimes \mathbf{U}_\alpha)\right) = \\ - \varepsilon_\alpha \nabla p_\alpha + \nabla \cdot \left(\varepsilon_\alpha \mu_\alpha (\nabla \mathbf{U}_\alpha + (\nabla \mathbf{U}_\alpha)^T)\right) + \mathbf{S}_{M\alpha} + \mathbf{M}_\alpha\end{aligned} \tag{3.2}$$

In the momentum equation, Equation 3.2, the terms on the left hand side are accumulation and convection respectively. The first term on the right-hand side is the pressure gradient and the second term describes the transport due to viscous forces. $\mathbf{S}_{M\alpha}$ is the source term taking into account the external body forces and user defined momentum sources. The forces acting on phase α due to presence of other phases is included in the term $\mathbf{M}_\alpha$. This will be explained in more detail below.

To close the equation system, two constraints are needed, the first one is that the volume fractions sum to unity.

$$\sum_{\alpha=1}^{N_p} \varepsilon_\alpha = 1 \tag{3.3}$$

The second constraint is that all phases share the same pressure field.

$$p_\alpha = p \quad \forall \quad \alpha = 1, ..., N_p \tag{3.4}$$

3.2 Momentum transfer

When more than one phase is present and the flow is considered in-homogeneous, the inter-phase momentum transfer occurs because of interfacial forces acting on each phase α due to interaction with phase β. The forces are equal and opposite and sum to zero and arise from independent physical phenomena such as, drag force, solid particle collisions etc.

The interphase drag force is generally expressed by,

$$\mathbf{M}_\alpha = c_{\alpha\beta}^{(d)} \Big(\mathbf{U}_\beta - \mathbf{U}_\alpha \Big) \tag{3.5}$$

in Equation 3.2, for the multiphase model utilized in this work, the drag coefficient is defined as follows:

$$\mathbf{D}_{\alpha\beta} = C_D \rho_\alpha A |\mathbf{U}_\beta - \mathbf{U}_\alpha| (\mathbf{U}_\beta - \mathbf{U}_\alpha) \tag{3.6}$$

where $\mathbf{D}_{\alpha\beta}$ is the total drag on phase β from phase α and A is the projected area of the body in the flow direction according to Ansys [38]. The total drag for this application is defined as:

$$\mathbf{D}_{\alpha\beta} = \frac{\varphi_\beta}{\varphi_\alpha} \left(R_1 \frac{\varphi_\beta}{\varphi_\alpha} + R_2 |U_\beta - U_\alpha| \right) \tag{3.7}$$

where the constants R_1 and R_2 are from equation 3.9 below.

The interaction between the solid particles present is modelled via the solid pressure. The model used is the one developed by Härkönen [14] which relates the solid pressure to a volume fraction.

$$\varphi_\beta = k_0 + P_s^{k_1}(k_2 + k_3 ln(\kappa)) \tag{3.8}$$

where κ is the kappa number which describes the degree of delignification. k_0 is a material constant which describes the critical point of volume fraction where enough solids are present to form a network as according to de Kretser et al [8] and, k_1, k_2 and k_3 are material constants related to the elasticity of the material. Härkönen [14] further describes the modified Ergun equation and the material specific constants R_1 and R_2 which model the permeability.

$$\frac{\Delta P}{\Delta l} = R_1 \frac{(1-\varphi_\beta)^2}{\varphi_\beta^3} v + R_2 \frac{(1-\varphi_\beta)}{\varphi_\beta^3} v^2, \tag{3.9}$$

the first term is the laminar term and represents the flow resistance due to viscous forces, the second term is flow resistance for "turbulent" flow, and φ_β is the void fraction.

3.3 Viscosity

Viscosity is a measure of the friction between particles, which are treated as a Bingham fluid, this implies that there is a threshold value of the force needed to disrupt the network of solids, as first implemented by Pougatch [33]. This is reasonable since one of the most significant characteristics of this matter of solid particles is the yield stress. On the macro level a large number of particles will behave as a solid until the yield stress is exceeded, and beyond that point, the particles will move as a highly viscous fluid.

$$\mu_{eff} = \mu + \frac{\tau_0}{\gamma} \tag{3.10}$$

where $\tau_0 = f(P_S)$ and γ is the shear strain rate.

3.4 Wall friction

The solid phase fluid interaction with the wall is analogous to the behavior of two non-deforming solids in contact. The solid phase fluid remains in rest until an applied stress exceeds the frictional stress between the wall and the solid phase. Above this critical stress, the solid phase fluids move along the wall. The French research group *Groupment de Recherche Miliuex Divisés, GDR MiDi* examined the velocity profiles of granular flow in six different configurations both experimentally and numerically, where the vertical chute is the most representative for the present application. GDR MiDi presented that for the vertical chute a velocity profile which exhibits a non-zero velocity at the walls, a shear region close to the walls and a plug flow region in the center. Pougatch et al.[33] used a model for the solid's behavior at the wall, in which it is possible for the solid phase to slip at the wall. The tangential yield stress is proportional to the solid pressure P_S. The interaction between the wall and the solids is similar to the behavior between the solids themselves. Pougatch et al. reason that it is fair to assume that the chips in the digester slip more easily against the digester walls than against each other, based on the surface roughness. After movement is initiated by exceeding the critical stress, the tangential stress at the wall is a function of the solid pressure P_S. The velocity at the wall is not resolved but modelled as a partial slip condition which transfers only the momentum into the fluid body.

$$\tau_{wall} = f_{wall} P_s \tag{3.11}$$

where f_{wall} is the friction coefficient.

Chapter 4

Ultrasound Velocity Profiling

In this section a short description of the basic physics of the ultrasound velocity measurement technique used will be given together with a brief review of previous applications of the measuring technique. The following theory section is based on Kossof [39] and Wiklund [40].

4.1 Ultrasound

The ultrasound velocity profiling technique is based on the Doppler effect, which according to Meola et al [41], is defined as,

> The doppler effect is the observed variation of frequency when a ultrasound pulse from a fixed source strikes moving particles in a vessel.

The following theory section is based on Kossof [39] and Wiklund [40]. To produce ultrasound waves a transducer converts mechanical energy to an oscillating wave of varying pressure using a piezoelectric material [42]. The physical properties of the transducer set the finite dimensions of the propagating ultrasound waves. Two main features of ultrasound are the velocity of propagation and acoustic impedance. Ultrasound waves propagate with different velocity depending on the medium, some examples of speed of sound are, in water approximately 1500 m/s, Greenspan and Tscheigg[43] in air 330 m/s, Wong [44] in stainless steel approximately 6000 m/s, Prohaska[45] and for pulp approximately 1500 m/s, Wiklund [46]. The low speed of sound in air is a major limiting factor to apply ultrasound velocity profiling to air filled structures. Air also has a low acoustic impedance, which is defined as $\rho \cdot v$ where ρ is the density of the medium and v is the speed of sound in the medium.

The difference in acoustic impedance between two materials determines how much energy that is reflected back as the ultrasound waves propagate from one material to another.

When performing an ultrasound velocity measurement, the transducer is placed at the outer walls of the equipment in question. To create the velocity profile a great number of ultrasound pulses are emitted into the fluid on the inside of the walls. During the time between the omitted pulses the transducer is switched to receiving mode, meaning that the echoes of the pulses are only sampled during small specific time slots, commonly denoted as gates. In each gate, the velocity is determined after signal processing by:

$$v_i = \frac{c \cdot f_i^{Doppler}}{2 f_0 cos\theta} \tag{4.1}$$

where c is the speed of sound for the medium, $f_i^{Doppler}$ the Doppler frequency shift for gate i, f_0 is the frequency of the emitted ultrasound and θ the doppler angle, as described by Wiklund et al [40]. According to Wiklund [40] the doppler angle θ is:

> the angle between the direction of the moving reflectors main velocity vector and the direction of the measuring line.

Wiklund et al [40] further discussed that to construct complete instantaneous velocity profiles the distance between the particles, surfaces which reflects the ultrasound pulses, somewhere along the measuring line and the transducer is determined by a time-of-flight measurement. The speed of sound, c for the current medium is known, together with the time t, between the transmitting and receiving the ultrasound pulse.

$$s = \frac{c \cdot t}{2} \tag{4.2}$$

A key feature which limits the measurement depth and maximal detectable velocity is the *pulse repetition frequency,* f_{prf}. Takeda [47] describes in detail the limitations and the correlations between these. The pulse repetition frequency, f_{prf} is the number of repetitions of a signal during a specific time transmitted by the transducer during a measurement. According to Takeda [47] the maximum depth of the ultrasound is determined by:

$$d_{max} = \frac{c}{f_{prf}} \tag{4.3}$$

To measure in large equipment a low f_{prf} is needed. Further, the Nyquist sampling theorem determines the upper limit of the measurable velocity, Takeda [47],

$$max(f_D) < f_{prf}/2, \qquad V_{max} < c f_{prf}/4 f_0 \tag{4.4}$$

where f_D is the Doppler frequency and f_0 is the basic frequency of the transducer. Equations 4.3 and 4.4 give that for a specific f_0 the maximum measurable

velocity decreases as the measurable depth increases due to the required lowering of the f_rpf. These constraints constitute a limiting tradeoff for the ultrasound velocity profiling method, Takeda [47];

$$V_{max}d_{max} < \frac{c^2}{8f_0} \tag{4.5}$$

In the case of high concentration of particles, scattering occurs which decreases the accuracy of the measurements, as found by Kotze et al. [48].

4.2 Previous Applications of Ultrasound Velocity profiling

A comprehensive review of the development of the ultrasound Doppler technique to measure two- and three-phase flow and all the contributions made to advance in the field has been presented by Tan et al. [49]. A further extensive review about the development of ultrasound profiling technique with focus on rheological properties was presented by Krishana et al. [50].

Several investigations on the behavior of viscoelastic fluids such as pulp have been conducted. Wiklund et al. [51] investigated the properties of the behavior near the wall and concluded that there is a sharp velocity gradient near the wall and a distinct plug in the center, which increases with higher concentration. Wiklund et al. [46] also investigated and compared Ultra Sound Velocity profiling to Laser Doppler Anemometry and found that both techniques successfully determined plug flow in highly concentrated pulp suspensions. Fock et al. [52] studied the behavior of pulp suspensions near pipe walls and found a sharp velocity gradient and, a distinct plug flow in the center. The data obtained from the ultrasound measurements also showed a concentration gradient, with lower concentration of fibers near the wall. Claesson et al. used UVP to examine the behavior of planar jets of pulp [53]. Haldenwang et al.[54] have applied the UVP technique to measure the viscous behavior of non-Newtonian fluids in a flume of width $0.3\,m$, they assumed that the velocity profiles are symmetric and measured over half the width of the flume and concluded that the method is applicable to measure viscous properties of non-Newtonian fluids. In 2008 Kotzé et al. [48] used ultrasound velocity profiling in-line combined with pressure difference measurements to measure rheological properties of non-Newtonian slurries of liquid and solid particles, in comparison to tube viscometry and conventional rheometry it was found that the agreement was within 15%. Three different materials were investigated, and in the most highly concentrated material, it was found that the ultrasonic energy was attenuated to a higher degree compared to the lower concentrations and the velocity profile was distorted, resulting in a less covered range of the pipe diameter.

Chapter 5

Results

In this section the results from the numerical simulations and the ultrasound velocity profiling will be presented.

5.1 Numerical Results

The focus of this work was to investigate the Eulerian multiphase flow models initially developed by Härkönen [14] and further extended by Pougatch [33] to determine the sensitivity of the output. By varying the most significant model parameters, it aims to show the importance of properly chosen material constants for the actual biomaterial handled in the current industrial equipment. Below is an abbreviated presentation of some of the parameters examined. For further details, see Paper I attached.

The computational domain is a 2D axisymmetrical representation of an existing impregnation vessel utilized at a mill. The vessel includes two screen packages, see Figure 1.1 at positions 2 and 3, where liquid is extracted and circulated, and two vertical positions of injection points, Figure 1.1, position 4 and 5, the chips are fed into the vessel at the top and 2 m above the screens is the liquid level, position 1, hence the impregnation vessel is not completely filled with liquid. The cooking liquid is fed into the vessel at the top and also at the two injection positions, which are placed around the spherical part of the bottom for the current geometry, to dilute the outflow. The upper injection point is located at the intersection of the spherical bottom and cylindrical upper part. The lower injection point is located at a radius of 3.2 $[m]$. The domain is limited to the liquid level of the equipment, where a pressure boundary condition describes the conditions at the top of the impregnation vessel. The outlet condition is a volumetric flow which is determined by the pump to the digester in the mill. Both screens and injections are modelled as source terms and the pump as a constant outlet velocity. The flow rates are specified in Table 5.1, and the geometry can be seen in Figure 1.1 with boundaries marked and additionally described in Section 1.2.

Boundary	Value	Units
Inlet	0	[Pa]
Oulet	0.5	$[m^3/s]$
Screens	0.025	$[m^3/s]$
Dilutions	0.1	$[m^3/s]$

Table 5.1: Boundary conditions.

The numerical simulations executed with ANSYS CFX 2022R1, are transient, with timestep $t = 0.001\,[s]$ and solved with the *High Resolution* numerical scheme. The mesh consists of $3 \cdot 10^4$ polyhedral cells with an average size of 0.2 m. Both phases are treated as continua, hence the particles are not individually resolved, the particle size is $d_p = 0.01\,[m]$.

The model constants for Equations 2.5, 3.9, and 3.11 used for the base case are presented in Table 5.2 and the variations for the abbreviated sensitivity analysis are presented in Table 5.3. The constants k_2 and k_3 were varied as a pair to alter the behavior of the solid pressure, Equation 2.5, the combinations will be termed as 'low' and 'high' and refer to the level of stiffness in the chips phase described by the solid pressure function. Each value is a significant deviation from the original model, but still of reasonable magnitude and numerically stable. The wall friction coefficient was varied separately.

Constant	Value	Units
k_0	0.64	—
k_1	0.59	—
k_2	0.83	—
k_3	0.14	—
κ	150	—
R_1	$4.6 \cdot 10^3$	$[kg/m^3 s]$
R_2	$3.9 \cdot 10^6$	$[\mathrm{kg/m^3}s]$
f_{Wall}	0.25	—

Table 5.2: Model constants of base case from Härkönen [14] and Pougatch [33].

Constant	Low value	High Value
k_2	1.53	0.45
k_3	0.26	0.075
f_{Wall}	0.125	0.4

Table 5.3: Model constants for sensitivity analysis.

In the examined impregnation vessel, an arch is formed between the internal conical structure and the walls of the vessel. The arch breaks and is rebuilt periodically as can be seen in Figure 5.1(a) and 5.1(b). A fixed volumetric flow rate is extracted by the pump at the bottom of the vessel, this is modelled

by applying a constant velocity as a boundary condition at the outlet. It can be seen that the pressure below the arch as it forms is lowered due to the constant extraction of material. As the arch breaks, the pressure rises. The arch is formed due to the material moving downwards because of gravity and the extraction by the pump. By monitoring the volume fraction of wood chips, the periodical formation of an arch can be seen, see Figure 5.1(a). The corresponding pressure during the simulation at the same points in the domain can be seen in Figure 5.1(b). In accordance with previous mentioned theory and discrete element model simulations by Yoshida [23], the periodicity is identical.

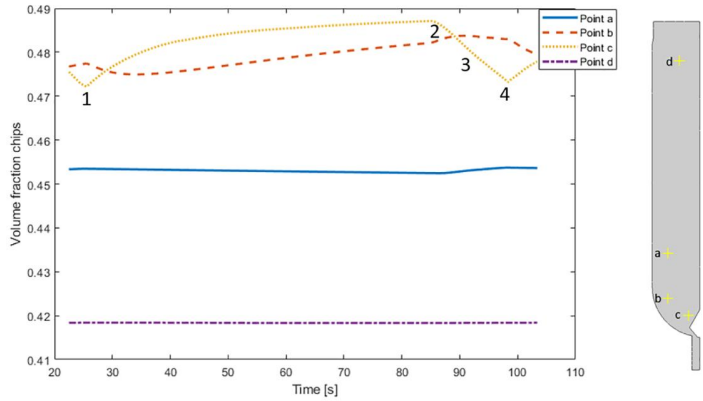

(a) Average volume fraction during arch formation and collapse. 1-No arch, 2-full arch, 3-arch collapse, 4-No arch, same as 1. Monitor points a-d marked in geometry.

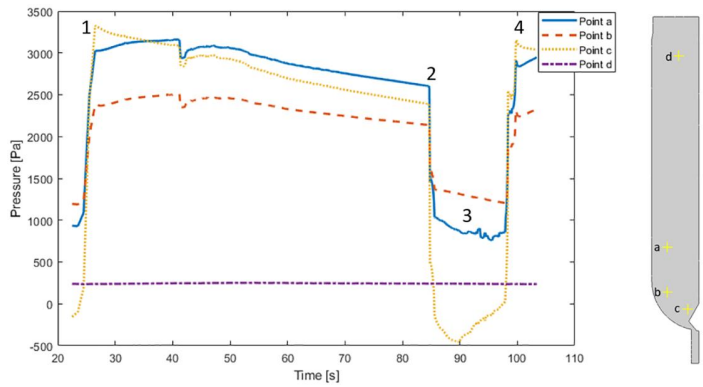

(b) Average pressure during arch formation and collapse. 1-No arch, 2-full arch, 3-arch collapse, 4-No arch, same as 1, corresponding to Figure 5.1(a). Monitor points a-d marked in geometry.

Figure 5.1: Volume fraction of wood chips and pressure during arch formation and collapse.

By varying the constants k_2 and k_3 in Equation 2.5, the function modelling the solid pressure, P_S has been examined. The values for the base case and their variations are presented in Tables 5.2 and 5.3, respectively. The solid pressure is incorporated in models that describe the interaction between the chips and the vessel, as well as the interaction between the chips themselves, the viscosity of the chips continuum. Altering the constants to correspond to a less stiff chips column also results in a decrease in both viscosity and the load-bearing capacity of the chip column against the vessel wall. Correspondingly, k_2 and k_3 can be altered to describe a stiffer and less deformable chips column. Figure 5.2(a) shows that a stiffer version of P_S leads to a less densely packed chip column, while a lower P_S results in a more densely packed column due to the greater influence of liquid flow on softer chips. The drag force is kept the same and a lower P_S thus leads to bridge formation at a higher volume fraction. Furthermore, a higher P_S results in a more uniform distribution of chips, both vertically and horizontally. Figure 5.2(b) indicates that the pressure drop is lower for higher P_S, which is expected due to the reduced volume fraction of chips at the bottom of the vessel. As long as the viscous forces of the wood chips column are not surpassed by other forces acting on the arch, such as gravity and hydraulic pressure, the formation and maintenance of arches are possible.

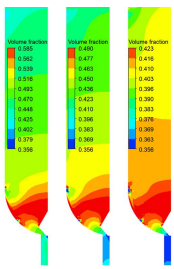

(a) Volume fraction of chips for three different pairs of k_2 and k_3. $k_2 = 1.54$ and $k_3 = 0.26$, $k_2 = 0.83$ and $k_3 = 0.14$, $k_2 = 0.45$ and $k_3 = 0.075$

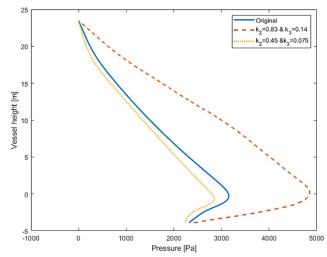

(b) Pressure profile through reactor r=R/2, for three different values of different pairs of k_2 and k_3.

Figure 5.2: Volume fraction of chips and pressure profiles for various solid pressure equations.

To examine the effect of the wall friction on the flow field of wood chips in the impregnation vessel, three values, as presented in Table 5.2 and 5.3 were examined. For the lower value, it can be noted that the pattern of the packing of the wood chips is similar to the pattern with the base case constant. In accordance with the Jansen effect, Mahajan et al [55], the actual level of packing is however higher, and explained by the fact that the wall carries less of the load of the wood chips column, causing it to settle more. With the higher wall fraction coefficient, the opposite is true, explained by the fact that the wall carried more of the load. The highest value reached is in the formation of an arch between the reactor wall and the cone structure inside the vessel, for all cases, see Figure 5.3(a). Altering the wall friction constant and thus the load carried by the wall has effects on how much the chips column settles and what the solid pressure in the column will be. The solid pressure is included in the model for the viscosity, and thus a higher friction between the walls also lowers the friction between the particles, resulting in a chips column which moves more easily and is less packed.

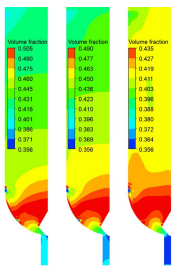

(a) Volume fractions of chips for for three different wall friction coefficients. From left: $f_W = 0.125$, $f_W = 0.25$, $f_W = 0.4$.

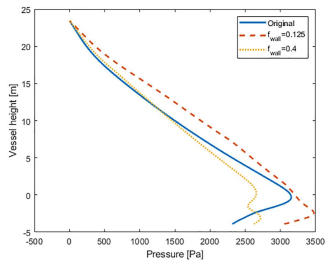

(b) Pressure profile through reactor at r=R/2, for three different wall friction coefficients.

Figure 5.3: Volume fraction of chips and pressure profiles for various wall friction coefficients.

5.2 Ultrasound Velocity Profiling Results

All measurements of the velocity profile in the impregnation vessel were conducted as a collaboration between Valmet, Incipientus and SCA Östrand. In standard operation mode, production rates range from approximately $80, [ton/h]$ to $110, [ton/h]$ and normal operational conditions within the mill lead to production fluctuations of up to 20% within a few hours. Therefore, a total measurement duration of 36 hours was deemed sufficient to assess the feasibility of the ultrasonic velocity profiling method for this application. For further details, see Paper II.

The transducer is connected to a Data Acquisition Box and a software which performs continuous velocity profile measurements, with each individual measurement taking approximately five minutes to complete. The transducer used has a base frequency of 1.25 MHz and features a piezoelectric element with a diameter of 2 inches. The maximum measurement depth is determined using Equation 4.3 with f_{prf} converted to seconds, 0.16, results in $d_{max} = 120\,m$ and the maximum detectable velocity is determined from Equation 4.4, the Nyquist criteria, $v_{max} = 2.35\,m$.

To ensure adequate acoustic coupling between the ultrasonic transducer and the steel wall of the vessel, a silicon heat sink compound was used as coupling paste, minimizing acoustic impedance mismatches. The transducer remained mounted on the vessel for approximately 36 hours, secured using a specialized rack designed to maintain consistent connection to the steel wall. The experimental setup used is depicted in Figure 5.4. The impregnation vessel is described in Section 1.2 The measurement point is positioned 3 m below the screen package, as illustrated in Figure 1.1, and at the measuring point the thickness of the walls of the impregnation vessel is 15 mm. The wood chips are characterized by an average length of approximately 25 mm, a width of 15 mm, and a thickness of 3 mm. Below the liquid level, the wood chips ideally become fully impregnated with the liquid. In this state, the density of the wood chips is estimated to $1150, [kg/m^3]$, while the density of the liquid is approximately $1000, [kg/m^3]$. Determining the precise local volume fraction within large-scale industrial equipment remains a challenge. The estimated volume fraction of wood chips varies between approximately 0.4 and 0.7 from the liquid level down to the bottom of the vessel. This estimate is derived from the load exerted by the column of wood chips, which is calculated using the equation for the solid pressure, Equation 2.5, presented in Section 3 and comparing it to Equation 5.1.

$$P_s = \Delta\rho \cdot g \cdot h \tag{5.1}$$

where ρ is the density of the wood chips, g the gravitational constant and h the height of the wood chips column.

Given the vessel diameter of $d = 8.8, m$ and an approximate density of atmospherically pre-steamed wood chips of $\rho_{chips} = 147, [kg/m^3]$, the average

velocity of the wood chips is estimated to be between 3.5 and 5.5, $[mm/s]$, calculated using the following Equation:

$$v_{chips} = \left(\frac{1000 \cdot Production}{\rho_C \zeta_d \zeta_{tot}} \cdot \frac{1}{\Psi} \right) \frac{1}{3600A} \tag{5.2}$$

where the production rate is expressed in air dry ton/h, ρ_C represents the density of dry wood chips, Ψ is the estimated packing degree of wood chips, and A denotes the cross-sectional area of the impregnation vessel, and ζ_d and ζ_{tot} are the yield in the pulp digester and mill total, respectively.

Figure 5.4: The transducer mounted to the impregnation vessel.

In Figures 5.5-5.6, some examples of Doppler spectra of the velocity from the measuring period of 36 hours are seen and show that it is possible to detect the velocity of the wood chips inside the impregnation vessel at ordinary process conditions which are also varying. The sensor was able to measure $\approx 350\,mm$ into the vessel after the wall. Shortly after $350\,mm$ the signal is severely attenuated, and no velocity is distinguishable. For all spectra it is noted that at the wall located at $x = 0\,m$ the velocity is non-zero followed by a steep gradient further away from the wall and beyond, there is plug flow established at $12.5\,mm$. Production data with 10-minute resolution, for 11-12 December 2024, is converted to velocity according to Equation 5.2 and presented in Figure 5.7 - 5.10 together with the UVP-data. Although the measurement depth is limited to below 10% of the radii of the impregnation vessel, the fluctuations of the production are captured when comparing the velocities. The lack of data seen in the curves for the measurements are due to bad quality measure-

ments with indistinguishable profiles. The average production velocity during the period for which the sensor was mounted ranged between $4.2 - 4.7\,mm/s$. As can be seen in Figures 5.5 and 5.6 the measured velocity is in the same range.

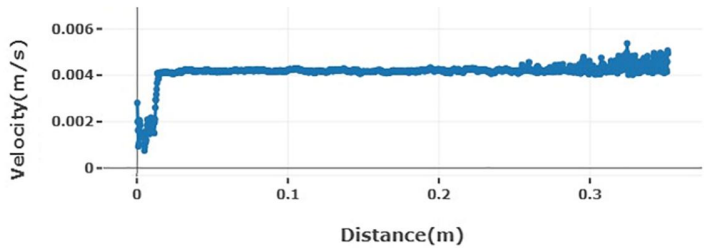

Figure 5.5: Velocity profile measured in impregnation vessel at 121224 04:04.

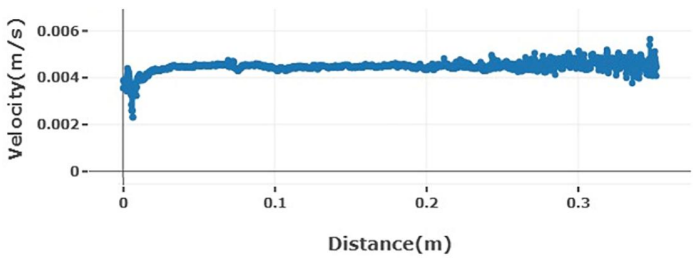

Figure 5.6: Velocity profile measured in impregnation vessel at 121224 16:18.

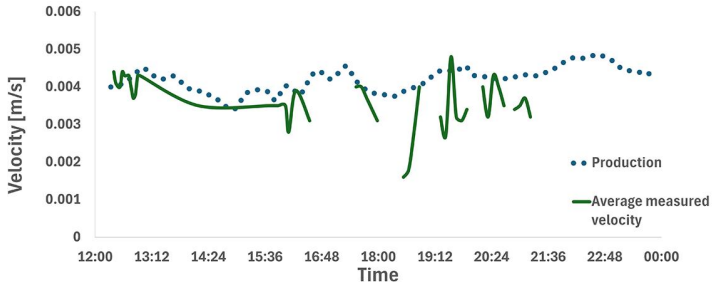

Figure 5.7: Production data for 111224 converted to velocity, shown together with average measured velocity.

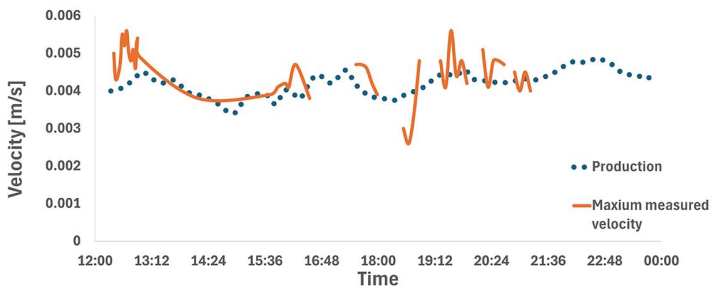

Figure 5.8: Production data for 111224 converted to velocity, shown together with maximum measured velocity.

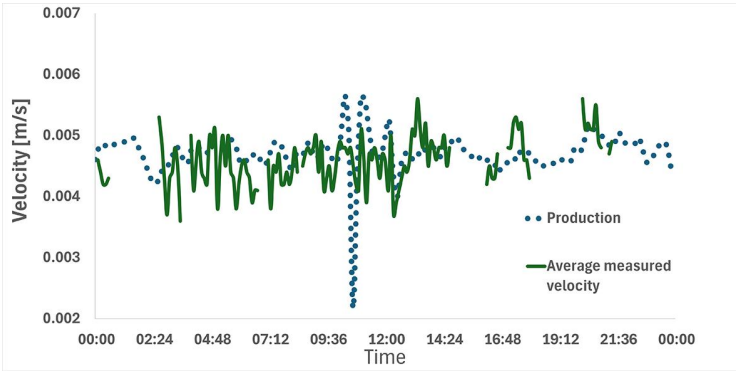

Figure 5.9: Production data for 121224 converted to velocity, shown together with average measured velocity.

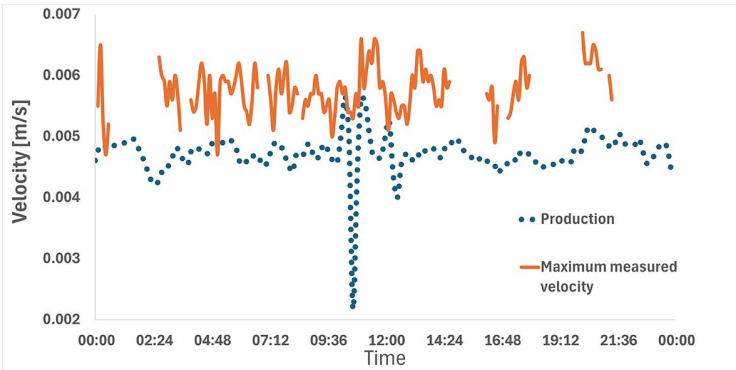

Figure 5.10: Production data for 121224 converted to velocity, shown together with maximum measured velocity.

Chapter 6

Discussion

An advantage of using the Eulerian continuum model approach is its ability to represent large-scale systems containing billions of particles while integrating heat and mass transport as well as chemical reactions, thus enabling comprehensive modelling of industrial pulping equipment. The model examined in this study is two-dimensional, with symmetrical geometry and boundary conditions. Introducing asymmetric boundary conditions or perturbations would necessitate a three-dimensional framework to capture these effects. The two-dimensional model exhibits greater stiffness due to its reduced degrees of freedom, which may lead to an overestimation of the arch formation. A three-dimensional model would introduce instabilities in the tangential direction, likely resulting in reduced packing of wood chips and the breakdown of structures prior to complete arch formation. Nevertheless, an important finding is that the model successfully captures phenomena previously observed in more refined models, such as the Discrete Element Method (DEM), when such effects are present.

The impregnation vessel examined in this study exhibits geometric similarities to silos used for the storage of agricultural materials and consequently experiences analogous physical phenomena. The formation and subsequent collapse of structural arches were observed in all variations in the parameter sensitivity analysis, suggesting a potential geometric concern. In both silos and impregnation vessels, the granular material is discharged from the bottom. However, a key distinction lies in the presence of a liquid medium in digesters as opposed to air in silos. This difference significantly influences the drag forces between solid components due to the disparity in density between air and liquid, which spans several orders of magnitude. As a result, minor velocity variations in the liquid medium induce more substantial changes in drag force at equivalent velocities. Since even small force variations can be transmitted to the solid phase, an increase in the packing of wood chips is observed. Small changes along the large length of the impregnation vessel sum up to significant effects.

Conversely, if the liquid moves counter currently to the solid phase, the packing of wood chips is reduced to a greater extent. Another important distinction is that silos for agricultural material often operate in batch mode, while the impregnation vessel is continuous, and an even flow of material is important.

A critical parameter for modelling the flow of wood chips is the solid pressure. Variations in the model constants, k_2 and k_3 demonstrated a significant influence on degree of packing of wood chips, aligning with the findings of Hinterreiter [22], who regarded it as a lumped parameter accounting for moisture content, particle shape, and aspect ratio. Wood chip distribution and packing is the primary determinant of liquid distribution and, consequently, the efficiency of the pulping process. A similar effect of the degree of packing can be noted when varying the wall friction coefficient, a higher wall friction coefficient, which corresponds to the wall carrying more of the load from the chips column, also results in a lower volume fraction in the bottom of the vessel. When comparing the results from the varying of the wall friction coefficient to the results from the solid pressure variation, the effect of the viscosity can be seen. A lower, P_S results in lowering the load that the wall can carry, and also makes the chips more easily packed, or less viscous, the combined effect can be noted when comparing the left most picture in Figures 5.2(a) and 5.3(a), where the volume fraction is higher in Figure 5.2(a). A lower viscosity results in an even higher volume fraction. Viscosity, which represents inter-particle friction, is only relevant when particle contact occurs, which corresponds to exceeding a critical particle volume fraction. Under such conditions, solid pressure is also present. In this study, the solid-phase viscosity is described using a Bingham model as a function of solid pressure and shear strain rate, since viscosity depends on solid pressure, variations in the volume fraction of wood chips inherently alter viscosity.

The appropriate selection of parameters based on the specific biomaterial properties is crucial during equipment design. The parameter study conducted in this research underscores the significance of correct material constants to avoid an underestimate or overestimate of equipment malfunctioning risks, such as operational irregularities and inefficient chemical distribution caused by excessive packing of wood chips.

Theoretical calculations of the maximum detectable velocity and measurement depth, as outlined in Section 4.1, indicate that it is theoretically possible to measure up to 120 m with the settings used for the impregnation vessel, based on Equations 4.3, 4.4, and 4.5. However, this theoretical value does not account for signal attenuation due to the steel vessel wall or the high particle loading, both of which severely impact signal penetration depth. Comparing the measured depth reached with the dimension of the wood chips, it is estimated that the measurement depth encompasses between 16 and 133 wood chips, depending on their ordering and orientation. Given the random distribution of chips, the true number likely falls within this range. Further analysis of measured velocities in relation to production rates reveals that for

a production rate of 93.5 tons per day, chip packing degrees of 1.3 and 1.4 correspond to average velocities of approximately 4.6 mm/s and 4.3 mm/s, respectively, representing a difference of approximately 7%. Implying that if the estimated degree of packing of wood chips is off by 7% the converted process data will not match the measured velocity with better accuracy. Degree of packing can, in principle, be estimated using a constitutive equation, provided that the relevant material parameters are known. However, in industrial environments, these parameters are often unavailable, complicating the estimation. Additionally, the volume fraction of wood chips is likely to fluctuate over time due to varying process conditions and operational factors, such as liquid level changes. Figures 5.7 - 5.10 indicate that certain converted process data align more closely with measured maximum velocities, while others better match measured average velocities, suggesting temporal variations in chip volume fraction. Furthermore, the moisture content of wood chips is unknown; while ideally saturated with liquid, incomplete pre-steaming could leave air within the chips, which would lead to attenuated ultrasound signals. The sensor was attached to the impregnation vessel using a custom bracket, but vessel vibrations posed challenges in securing the sensor, as minor displacement could affect sensor coupling with the vessel wall, thereby impacting measurement depth.

Chapter 7

Conclusions

The Euler-Euler model examined in this study captures the periodic behavior of arch formation and breakage, as well as the corresponding hydraulic pressure variations. These phenomena have previously been observed in smaller systems modelled using the discrete element model (DEM) with a limited number of particles. The present model of an industrial-scale impregnation vessel demonstrates its capability to describe large-scale granular flow of wood chips. It captures the occurrence of formation of arches despite not resolving each individual particle, which is not feasible for the size of industrial cooking system equipment. An accurate flow field is a key feature for understanding the operation of equipment in cooking systems. This possibility opens for further model development including heat and mass-transfer for a full-scale investigation tool of industrial scale vessels with particle flow.

Despite the extremely high particle loading within the impregnation vessel, this study demonstrates the potential of Ultrasonic Velocity Profiling, UVP, to visualize the velocity of wood chips inside the vessel. A significant advantage of this method is its ability to perform measurements through the 15 mm thick steel wall, confirming that UVP is a truly non-invasive technique. This opens to possibilities for measuring flow characteristics under conditions that are otherwise highly challenging to access in industrial equipment.

Given the inherent uncertainties associated with the process, the ability to capture the overall flow behavior and estimate reasonable velocity distributions supports the conclusion that UVP has potential as a viable method for obtaining insight into the flow conditions of wood chips inside large-scale industrial impregnation vessels.

The velocity profiles obtained near the vessel wall exhibit non-zero velocities, which is consistent with the expected behavior of a dense granular flow. A thin shear layer is observed, while the remaining profile exhibits plug flow characteristics. These measurements suggest that the flow of wood chips at an industrial scale can be regarded as a dense granular flow. Furthermore, the measurements support the assumption that the viscosity can be modelled using a first order approach such as a Bingham fluid, for computational fluid dynamics (CFD) simulations of the system.

Chapter 8

Future work

The CFD-model based on the Eulerian approach, of the impregnation vessel can be extended to include the heat- and mass transport occurring due to the chemical reactions of the delignification process, which is the next step in the cooking process in pulp mills. Including the chemical reactions gives a full-scale model of the cooking system. It is of high importance when extending the model with the heat and mass transport to ensure that the limiting coefficients of the reactions and diffusion trough and in the two present phases are in the right order of magnitude and experimental work regarding this is needed. Such a full-scale model could be used by the industry to design and optimize the cooking system.

This continuum model of wood chips can capture several important phenomena and could be supplemented with experimental data for the wood of interest to obtain a good modeling tool.

Ultrasound velocity profiling has shown potential to gaining insight in the flow conditions in industrial equipment. Further development of the technique could result in a larger measurement depth and detection of possible irregularities in the flow field. Further measurements near the wall could have potential to detect concentration gradients as well.

Bibliography

[1] 'Sweden's forest industry in brief.' (), [Online]. Available: https://www.forestindustries.se/forest-industry/statistics/facts-and-figures/. (accessed: 03.11.2025) (cit. on p. 1).

[2] M. Kassbereg, *Sulfatmassa tillverkning, Bok 1.* Skogsindustrins Utbildning i Markaryd, 1998 (cit. on p. 2).

[3] C. S. Campbell *et al.*, 'Rapid granular flows,' *Annual Review of Fluid Mechanics*, vol. 22, no. 1, pp. 57–90, 1990 (cit. on pp. 10, 11).

[4] G. M. gdrmidi@ polytech. univ-mrs. fr http://www. lmgc. univ-montp2. fr/MIDI/, 'On dense granular flows,' *The European Physical Journal E*, vol. 14, pp. 341–365, 2004 (cit. on p. 10).

[5] P. Jop, Y. Forterre and O. Pouliquen, 'A constitutive law for dense granular flows,' *Nature*, vol. 441, no. 7094, pp. 727–730, 2006 (cit. on p. 10).

[6] D. M. Mueth, G. F. Debregeas, G. S. Karczmar, P. J. Eng, S. R. Nagel and H. M. Jaeger, 'Signatures of granular microstructure in dense shear flows,' *Nature*, vol. 406, no. 6794, pp. 385–389, 2000 (cit. on p. 10).

[7] D. M. Mueth, 'Measurements of particle dynamics in slow, dense granular couette flow,' *Physical Review E*, vol. 67, no. 1, p. 011 304, 2003 (cit. on p. 10).

[8] R. G. De Kretser, D. V. Boger and P. J. Scales, 'Compressive rheology: An overview,' *Rheology Reviews*, pp. 125–166, 2003 (cit. on pp. 11, 21).

[9] C. W. MacMinn, E. R. Dufresne and J. S. Wettlaufer, 'Fluid-driven deformation of a soft granular material,' *Physical Review X*, vol. 5, no. 1, p. 011 020, 2015 (cit. on p. 12).

[10] D. R. Hewitt, J. S. Nijjer, M. G. Worster and J. A. Neufeld, 'Flow-induced compaction of a deformable porous medium,' *Physical Review E*, vol. 93, no. 2, p. 023 116, 2016 (cit. on p. 12).

[11] Y. Gan and M. Kamlah, 'Discrete element modelling of pebble beds: With application to uniaxial compression tests of ceramic breeder pebble beds,' *Journal of the Mechanics and Physics of Solids*, vol. 58, no. 2, pp. 129–144, 2010 (cit. on p. 13).

[12] W.-F. Chen and G. Y. Baladi, *Soil plasticity: theory and implementation.* Elsevier, 1985 (cit. on p. 14).

[13] G. Pettersson and P. Pettersson, *Behavior and modeling of wood chips: experiments, constitutive relations and finite element modeling*. 2000 (cit. on p. 14).

[14] E. Härkönen, 'A mathematical model for two-phase flow in a continuous digester,' *Tappi journal*, vol. 70, no. 12, pp. 122–126, 1987 (cit. on pp. 14, 17, 18, 21, 27, 28).

[15] Q. F. Lee, 'Fluid flow through packed columns of cooked wood chips,' Ph.D. dissertation, University of British Columbia, 2002 (cit. on p. 15).

[16] M Alaqqad, C. Bennington and D. Martinez, 'The permeability of wood-chip beds: The effect of compressibility,' *The Canadian Journal of Chemical Engineering*, vol. 90, no. 5, pp. 1278–1288, 2012 (cit. on p. 15).

[17] T. Lundström, S. Toll and J. Håkanson, 'Measurement of the permeability tensor of compressed fibre beds,' *Transport in Porous Media*, vol. 47, no. 3, pp. 363–380, 2002 (cit. on p. 15).

[18] J. Weitzenböck, R. Shenoi and P. Wilson, 'Measurement of three-dimensional permeability,' *Composites Part A: Applied Science and Manufacturing*, vol. 29, no. 1-2, pp. 159–169, 1998 (cit. on p. 16).

[19] R Djebbar, S. Beale and M. Sayed, 'Multi-phase granular flow in a reactor,' 1999 (cit. on p. 16).

[20] A Drescher, A. Waters and C. Rhoades, 'Arching in hoppers: I. arching theories and bulk material flow properties,' *Powder Technology*, vol. 84, no. 2, pp. 165–176, 1995 (cit. on p. 17).

[21] R. Hidalgo, C Lozano, I Zuriguel and A Garcimartín, 'Force analysis of clogging arches in a silo,' *Granular Matter*, vol. 15, no. 6, pp. 841–848, 2013 (cit. on p. 17).

[22] S. Hinterreiter, H. Hartmann and P. Turowski, 'Method for determining bridging properties of biomass fuels—experimental and model approach,' *Biomass conversion and Biorefinery*, vol. 2, no. 2, pp. 109–121, 2012 (cit. on pp. 17, 40).

[23] J. Yoshida, 'An analytical study on the pulsation phenomenon of granular materials in silos during discharge,' *Advanced Powder Technology*, vol. 5, no. 1, pp. 85–98, 1994 (cit. on pp. 17, 29).

[24] K. To, P.-Y. Lai and H. Pak, 'Jamming of granular flow in a two-dimensional hopper,' *Physical review letters*, vol. 86, no. 1, p. 71, 2001 (cit. on p. 17).

[25] J. Saltin, 'A predictive dynamic model for continuous digesters,' in *Tappi pulping conference*, TAPPI PRESS, 1992, pp. 261–261 (cit. on p. 17).

[26] F. A. Michelsen and B. A. Foss, 'A comprehensive mechanistic model of a continuous kamyr digester,' *Applied mathematical modelling*, vol. 20, no. 7, pp. 523–533, 1996 (cit. on pp. 17, 18).

[27] T. Christensen, 'A mathematical model of the kraft pulping process,' 1982 (cit. on p. 17).

[28] P. A. Wisnewski, F. J. Doyle III and F. Kayihan, 'Fundamental continuous-pulp-digester model for simulation and control,' *AIChE journal*, vol. 43, no. 12, pp. 3175–3192, 1997 (cit. on p. 17).

[29] N. C. Fernandes and J. A. Castro, 'Steady-state simulation of a continuous moving bed reactor in the pulp and paper industry,' *Chemical engineering science*, vol. 55, no. 18, pp. 3729–3738, 2000 (cit. on p. 17).

[30] S. Bhartiya, P. Dufour and F. J. Doyle III, 'Fundamental thermal-hydraulic pulp digester model with grade transition,' *AIChE Journal*, vol. 49, no. 2, pp. 411–425, 2003. DOI: 10.1002/aic.690490212. eprint: https://aiche.onlinelibrary.wiley.com/doi/pdf/10.1002/aic.690490212. [Online]. Available: https://aiche.onlinelibrary.wiley.com/doi/abs/10.1002/aic.690490212 (cit. on p. 17).

[31] B. Pourian, 'Analyzing the hydro dynamics and the chemical reactions in pulp digester systems using cfd modelling,' Ph.D. dissertation, Mälardalen University, 2011 (cit. on p. 18).

[32] P He, M Salcudean, I Gartshore and E Bibeau, 'Modeling of kraft two-phase digester pulping processes,' in *Process and Product Quality Conference and Trade Fair*, vol. 3, 1999, pp. 1407–1418 (cit. on p. 18).

[33] K Pougatch, M Salcudean and I Gartshore, 'A numerical model of the reacting multiphase flow in a pulp digester,' *Applied mathematical modelling*, vol. 30, no. 2, pp. 209–230, 2006 (cit. on pp. 18, 21, 22, 27, 28).

[34] Y. Fan, 'Numerical investigation of industrial continuous digesters,' Ph.D. dissertation, University of British Columbia, 2005 (cit. on p. 18).

[35] R. A. A. Rantanen, *Modelling and control of cooking degree in conventional and modified continuous pulping processes*. 2006, vol. 68 (cit. on p. 18).

[36] R. R. Gustafson, C. A. Sleicher, W. T. McKean and B. A. Finlayson, 'Theoretical model of the kraft pulping process,' *Industrial & Engineering Chemistry Process Design and Development*, vol. 22, no. 1, pp. 87–96, 1983 (cit. on p. 18).

[37] S. Laakso *et al.*, *Modeling of chip bed packing in a continuous kraft cooking digester*. Teknillinen korkeakoulu, 2008 (cit. on p. 18).

[38] *Ansys cfx-solver theory guide*, ANSYS, Canonsburg, PA, 2024 (cit. on p. 20).

[39] G. Kossoff, 'Basic physics and imaging characteristics of ultrasound,' *World journal of surgery*, vol. 24, no. 2, pp. 134–142, 2000 (cit. on p. 23).

[40] J. Wiklund, I. Shahram and M. Stading, 'Methodology for in-line rheology by ultrasound doppler velocity profiling and pressure difference techniques,' *Chemical Engineering Science*, vol. 62, no. 16, pp. 4277–4293, 2007 (cit. on pp. 23, 24).

[41] M. Meola, J. Ibeas, G. Lasalle and I. Petrucci, 'Basics for performing a high-quality color doppler sonography of the vascular access,' *The Journal of Vascular Access*, vol. 22, no. 1_suppl, pp. 18–31, 2021 (cit. on p. 23).

[42] H. Thomann, 'Piezoelectric ceramics,' *Advanced Materials*, vol. 2, no. 10, pp. 458–463, 1990 (cit. on p. 23).

[43] M. Greenspan and C. E. Tschiegg, 'Speed of sound in water by a direct method,' *Journal of Research of the National Bureau of Standards*, vol. 59, no. 4, pp. 249–254, 1957 (cit. on p. 23).

[44] G. S. K. Wong, 'Speed of sound in standard air,' *The Journal of the Acoustical Society of America*, vol. 79, no. 5, pp. 1359–1366, May 1986, ISSN: 0001-4966. DOI: 10.1121/1.393664. eprint: https://pubs.aip.org/asa/jasa/article-pdf/79/5/1359/12233892/1359_1_online.pdf. [Online]. Available: https://doi.org/10.1121/1.393664 (cit. on p. 23).

[45] M Prohaska, M Panzenboeck, H Anderl and W Kordasch, 'Influence of chemical composition and microstructural parameters on speed of sound of various materials used for high-pressure applications,' in *18th World Conference on Nondestructive Testing, Durban, South Africa*, 2012, pp. 16–20 (cit. on p. 23).

[46] J. A. Wiklund, M. Stading, A. J. Pettersson and A. Rasmuson, 'A comparative study of uvp and lda techniques for pulp suspensions in pipe flow,' *AIChE Journal*, vol. 52, no. 2, pp. 484–495, 2006 (cit. on pp. 23, 25).

[47] Y. Takeda, 'Velocity profile measurement by ultrasonic doppler method,' *Experimental thermal and fluid science*, vol. 10, no. 4, pp. 444–453, 1995 (cit. on pp. 24, 25).

[48] R. Kotze, R. Haldenwang and P. Slatter, 'Rheological characterization of highly concentrated mineral suspensions using ultrasound velocity profiling with combined pressure difference method,' *Applied Rheology*, vol. 18, no. 6, pp. 62 114–1, 2008 (cit. on p. 25).

[49] C. Tan, Y. Murai, W. Liu, Y. Tasaka, F. Dong and Y. Takeda, 'Ultrasonic doppler technique for application to multiphase flows: A review,' *International Journal of Multiphase Flow*, vol. 144, p. 103 811, 2021 (cit. on p. 25).

[50] S. Krishna, G. Thonhauser, S. Kumar, A. Elmgerbi and K. Ravi, 'Ultrasound velocity profiling technique for in-line rheological measurements: A prospective review,' *Measurement*, vol. 205, p. 112 152, 2022, ISSN: 0263-2241. DOI: https://doi.org/10.1016/j.measurement.2022.112152. [Online]. Available: https://www.sciencedirect.com/science/article/pii/S0263224122013483 (cit. on p. 25).

[51] J. Wiklund, H. Fock, A. Rasmuson and M. Stading, 'Near wall studies of pulp suspension flow,' in *Proc. Int. Symp. on Ultrasonic Doppler Methods for Fluid Mechanics and Fluid Engineering*, 2001 (cit. on p. 25).

[52] H. Fock, J. Wiklund and A. Rasmuson, 'Ultrasound velocity profile (uvp) measurements of pulp suspension flow near the wall,' *Journal of Pulp and Paper Science (JPPS)*, vol. 35, no. 1, pp. 26–33, 2009 (cit. on p. 25).

[53] J. Claesson, A. Rasmuson, J. Wiklund and T. Wikström, 'Measurement and analysis of flow of concentrated fiber suspensions through a 2-d sudden expansion using uvp,' *AIChE Journal*, vol. 59, no. 3, pp. 1012–1021, 2013 (cit. on p. 25).

[54] R. Haldenwang, R. Kotzé and R. Chhabra, 'Determining the viscous behavior of non-newtonian fluids in a flume using a laminar sheet flow model and ultrasonic velocity profiling (uvp) system,' *Journal of the Brazilian Society of Mechanical Sciences and Engineering*, vol. 34, pp. 276–284, 2012 (cit. on p. 25).

[55] S. Mahajan, M. Tennenbaum, S. Pathak *et al.*, 'Reverse janssen effect in narrow granular columns,' *Physical Review Letters*, vol. 124, Mar. 2020. DOI: 10.1103/PhysRevLett.124.128002 (cit. on p. 32).